Revised chronology of northwest Laurentide ice-sheet deglaciation from ^{10}Be exposure ages on boulder erratics

Alberto V. Reyes[a,*], Anders E. Carlson[b], Glenn A. Milne[c], Lev Tarasov[d], Jesse R. Reimink[e], Marc W. Caffee[f]

[a]Department of Earth and Atmospheric Sciences, University of Alberta, Edmonton, AB, Canada
[b]Oregon Glaciers Institute, Corvallis, OR, USA
[c]Department of Earth and Environmental Sciences, University of Ottawa, ON, Canada
[d]Department of Physics and Physical Oceanography, Memorial University, NL, Canada
[e]Department of Geosciences, The Pennsylvania State University, University Park, PA, USA
[f]Department of Physics, Purdue University, West Lafayette, IN 47907, USA
*Corresponding author: areyes@ualberta.ca

ABSTRACT: We present new ^{10}Be surface exposure ages from boulders on bedrock to directly date northwest Laurentide ice-sheet deglaciation through a wide swath of the western Canadian Shield that had no previous reliable temporal constraints on ice-margin retreat. Uplift-corrected boulder ^{10}Be surface exposure ages are 13.9±0.2 ka (n=6) at a site on the western edge of the Slave Craton and 12.4±0.2 ka (n=5, 1 outlier) at a second site ~110 km up-ice to the east. These direct ^{10}Be ages for ice-margin retreat are ~2.4 kyr and ~1.6 kyr older, respectively, than the canonical deglacial chronology for the northwest Laurentide ice sheet that is based on minimum-limiting ^{14}C dates. We infer an ice-margin retreat rate of 60-100 m yr^{-1} between the two sites over an interval spanning the transition from the Allerød warm period into the Younger Dryas cold period. This is significantly slower than the rapid >800 m yr^{-1} retreat rate for the northwest Laurentide ice sheet inferred from earlier deglacial chronologies, which has been hypothesized as a potential source of meltwater forcing for the Younger Dryas cold period.

These first direct ages on spatio-temporal patterns of deglaciation in this data-poor region suggest that additional refinement of the deglacial chronology is needed to test hypotheses on the relation between ice-sheet retreat, associated meltwater discharge, abrupt climate change, and rapid sea-level rise.

Keywords: Pleistocene; glaciology; North America; cosmogenic isotopes; Laurentide Ice Sheet; last deglaciation; Canadian Shield

1. INTRODUCTION

The Laurentide ice sheet was the largest of the boreal ice sheets during the last glaciation (Clark et al., 2009; Lambeck et al., 2017). Deglacial meltwater from the Laurentide ice sheet has been implicated as a potential cause for abrupt cooling at the onset of the Younger Dryas (e.g., Johnson & McClure, 1976; Rooth, 1982; Broecker et al., 1989; Smith and Fisher, 1993; Carlson et al., 2007a; Murton et al., 2010; Leydet et al., 2018). In particular, the northwest sector of the Laurentide ice sheet (Fig. 1A) is a key sector in evaluating sources and timelines of meltwater flux, with various hypotheses linking meltwater and proglacial-lake runoff into the Arctic Ocean to subsequent weakening of the Atlantic meridional overturning circulation and, in turn, the onset of Younger Dryas cooling (Tarasov & Peltier, 2005; 2006; Murton et al., 2010; Condron & Winsor, 2012; Keigwin et al., 2018; Love et al, 2021; Norris et al., 2021).

Despite the importance of this sector in assessing the role of meltwater in abrupt climate change during the last deglaciation, a detailed chronological reconstruction for the deglaciation of the northwest Laurentide ice sheet is at best scant, and in most places is absent (Bryson et al., 1969; Dyke & Prest, 1987; Dyke, 2004; Dalton et al., 2020). Inland from the Arctic Ocean coastlines, where abundant ^{14}C shell ages exist (albeit with substantial caveats related to ^{14}C reservoir effects; e.g., Dyke, 2004; McNeely et al., 2006; Carlson & Clark, 2012), only about a dozen published ^{14}C dates—all of which provide only minimum-limiting ages for deglaciation—constrain the timing of northwest Laurentide ice-sheet margin retreat across the vast western

Canadian Shield (Figs. 1A, 1B; Dyke et al., 2003; Dalton et al., 2020). In this paper, we address the poorly constrained deglacial chronology for the northwest Laurentide ice-sheet deglaciation with new ^{10}Be surface exposure ages from erratic boulders on bedrock at two sites on the westernmost Canadian Shield.

2. METHODS

Following prior methods used for ^{10}Be surface exposure dating of Laurentide ice-sheet retreat on the eastern Canadian Shield (Carlson et al., 2007b; Ullman et al., 2016; Leydet et al., 2018), we sampled the surfaces of boulder erratics resting on local bedrock highs above any potential proglacial lake limits (e.g., Lemmen et al., 1994) that could have initially covered the boulders (Fig. 1C, D). This approach minimizes the potential for boulder exhumation from a fine-grained sediment matrix or for downhill rolling of the boulder after deposition, processes that would lead to exposure ages younger than ice retreat. We sampled six boulders at each of the two sites (Fig. 1A, B) along the reconstructed southeast-trending retreat path (Dyke, 2004) of the northwest Laurentide ice sheet across the Slave Craton of the western Canadian Shield. Bedrock geology in the region of both sites is dominated by Archean basement gneisses and granitoids with minimal Quaternary drift cover. The western site B16-1 (65.10 °N, 115.72 °W, 470 m above sea level.) is adjacent to the 10.0 ^{14}C ka (~11.5 cal ka) isochrone of Dyke (2004) (Fig. 1B). The sampling site is an ~150x50 m low-relief summit of bare bedrock, standing ~70 m above the surrounding terrain and an unnamed lake (Fig. 1C), upon which rest dozens of large erratic boulders (Fig. S1). The eastern site B16-2, ~110 km further in the direction of ice retreat, is on an island in central Point Lake (65.27 °N, 113.27 °W, 400 m above sea level) and is just east of the 9.5 ^{14}C ka (~10.8 cal ka) isochrone of Dyke (2004) (Fig. 1B). Samples were collected from boulders spread over several hundred square meters on the crest of the highest hill on the island (Fig. S2).

At University of Alberta, samples were crushed and sieved to obtain a 250-500 μm size-fraction, followed by magnetic separations to reduce non-quartz minerals. At PRIME Lab of

Purdue University, a final quartz purification was done following Kohl & Nishiizumi (1992). Purified quartz was dissolved in the presence of a low background ^{9}Be carrier ($^{10}Be/^{9}Be<10^{-15}$), with the purified BeO loaded into stainless steel cathodes and analyzed by accelerator mass spectrometry following Sharma et al. (2000). Measured $^{10}Be/^{9}Be$ ratios were normalized to primary standards ($^{10}Be/^{9}Be=2.85x10^{-12}$) prepared by K. Nishiizumi (Nishiizumi et al., 2007). Isotope ratios, samples masses, carrier amounts, and blank correction are shown in Table S1.

Ages were calculated using the base Arctic ^{10}Be production rate (Young et al., 2013) and the Lal/Stone time-varying scaling (Balco et al., 2008) (Table 1). Exposure ages calculated using the LSD scaling scheme (Lifton et al., 2014) are ~50-70 years older than those calculated using the Lal/Stone scheme (Table S1). Following Cuzzone et al. (2016) and Ullman et al. (2016), we calculated the mean-square weighted deviation (MSWD) to identify the appropriate method of calculating the sample mean and uncertainty, where a MSWD >1 prompts an arithmetic mean ± standard error while a MSWD <1 prompts an inverse-error-weighted mean ± uncertainty. All radiocarbon dates discussed here were calibrated with INTCAL 2020 (Reimer et al., 2020) and CALIB 8.2 (Stuiver et al., 2020), and presented as 1-σ calibrated age ranges or, for the Dyke (2004) isochrones, as calendar years ago.

The sampling sites have experienced significant (>400 m) post-glacial isostatic uplift (Peltier et al., 2015; Lambeck et al., 2017), which we account for when calculating surface exposure ages (Cuzzone et al., 2016; Ullman et al., 2016; Leydet et al., 2018; Jones et al., 2019; Carlson, 2020). Here, we test multiple earth model viscosity parameters using the ice sheet model of Lambeck et al. (2017) to determine their impact on the resulting isostatic uplift correction (Fig. 2A, B). The earth model viscosity profiles are defined by three parameters: lithosphere thickness (LT; km), upper mantle viscosity (UMV; 10^{21} Pa·s) and lower mantle viscosity (LMV; 10^{21} Pa·s), with the upper-lower mantle boundary at a depth of 670 km. The nine models are defined and identified by these three values in the sequence LT-UMV-LMV: 96-0.3-10; 96-0.3-30; 96-0p5-10; 96-0.8-10; 96-0.8-30; 120-0.3-10; 120-0.3-30; 120-0.8-10;

120-0.8-30. These viscosity profiles were chosen based on the uncertainty ranges given in Lambeck et al. (2017). The ice-sheet loading history is intimately tied to the Dyke (2004) deglacial isochrones, so we also explore the impacts of loading history on isostatic rebound using a suite of North American ice-sheet model simulations from Tarasov et al. (2012) that force a single VM5a earth viscosity model (Fig. 2C, D). Because the Tarasov et al. (2012) simulations were partly forced with the isochrones of Dyke (2004), we take an iterative approach and first calculate ^{10}Be ages using the Lambeck et al. (2017) and Tarasov et al. (2012) uplift corrections and then modify the isochrones of Dyke (2004) with the new chronology. This new regional chronology is subsequently used in two new ice-sheet model simulations that otherwise follow Tarasov et al. (2012). The resulting ice-sheet simulations are only applicable to the northwest Laurentide ice sheet and we assess their validity against modern-day uplift rates (Peltier et al., 2015) at Yellowknife, ~300 km south of the study sites. We average the isostatic uplift corrections, at 500-yr time slices, from these last two simulations as our best estimate of the time-averaged postglacial uplift at the sample sites (Fig. 2E, F).

3. RESULTS

The nine different earth viscosity parameter sets (Fig. 2A, B) and eight different ice-sheet histories, including the two new histories that are shown in red on Fig. 2C and D, yield isostatic uplift corrections that fall within a range of several tens of meters, with no large differences apparent when comparing variations associated with varying earth versus ice input parameters (Fig. 2E, F). At the western B16-1 site, corrections range from 76 m to 113 m (mean±s.d. = 94±14 m) with the two new ice-sheet model simulations giving a mean correction of 111 m (Fig. 2C, E). The correction is marginally smaller at the eastern B16-2 site due to its later deglaciation, ranging from 71 m to 109 m (mean±s.d. = 87±11 m) and a mean correction of 97 m for the two new ice-sheet model simulations (Fig. 2D, F). Our uncertainty range in potential uplift corrections is similar in magnitude to typical uncertainties in GPS-based field elevation measurements at boulder sampling sites; neither uncertainty is included in the calculated exposure age. The two new ice-sheet model simulations forced with revised, earlier ages for deglacial isochrones produce modern uplift rates of 4.9 and 4.6 mm yr^{-1} at Yellowknife (62.49 °N, 114.48 °W), consistent with geodetic observations of uplift at that site (4.8 ± 1.5 mm yr^{-1}, Argus et al., 2010; 6.1 ± 1.1 mm yr^{-1}, Peltier et al., 2015).

Uplift-corrected ^{10}Be ages at the western B16-1 site range from 13.6±0.6 ka to 14.4±0.5 ka (Fig. 3A) with a MSWD of 0.35, yielding an error-weighted mean and uncertainty of 13.9±0.2 ka (n=6) (Fig. 3B). The eastern B16-2 site has uplift-corrected ^{10}Be ages of 7.8±2.4 ka to 12.8±0.5 ka (Table 1); the boulder sample with the ~7.8 ka ^{10}Be age had low quartz recovery and poor AMS counting statistics (sample JR16-226; Table 1), and is rejected as both an analytical and geomorphic outlier. With the outlier removed, uplift-corrected ages at the eastern B16-2 site range from 12.1±0.6 ka to 12.8±0.5 ka (Fig. 3A) with a MSWD of 0.26, yielding an error-weighted mean and uncertainty of 12.4±0.2 ka (n=5, 1 outlier) (Fig. 3B). Including the ^{10}Be production rate uncertainty of ±3.8% (Young et al., 2013) yields propagated uncertainties of ±0.6 and ±0.5 kyr for, respectively, the site B16-1 and B16-2 weighted-mean exposure ages for deglaciation. Given site mean age uncertainties, we calculate a range in retreat rates over the ~110 km between the two sites of 60 to 100 km kyr^{-1} (Fig. 3C).

4. DISCUSSION & IMPLICATIONS

There are only 12 published ^{14}C dates pertaining to northwest Laurentide ice-sheet deglaciation within a 250 km radius of the B16-1 and B16-2 boulder sampling sites (Fig. 1). Of these, the nearest is a date of 7.5–8.2 cal ka BP on archeological charcoal at Acasta Lake, ~35 km north of site B16-1. The only other nearby ^{14}C-dated sites within 250 km provide minimum-limiting ages from gyttja and plant macrofossils in lake sediment (Moser & MacDonald, 1990; McNeely & McCuaig, 1991; Upiter et al., 2014; Crann et al., 2015; Dalton et al., 2020), with the oldest age of 9.3–9.7 cal ka BP on degraded wood found on an esker surface (Dredge et al., 1995). All these minimum-limiting calibrated ^{14}C ages are at least ~3 kyrs younger than the uplift-corrected deglaciation age for the eastern B16-2 site. This is similar to large temporal lags between ^{10}Be ages and post-glacial ^{14}C dates on the eastern Canadian Shield in Quebec and Labrador (Carlson et al., 2007b; Ullman et al., 2016) and the western Canadian Plains (Norris et al., in press), and illustrates the challenge of inferring deglacial ice-sheet chronologies from basal lake sediment dates.

The ^{10}Be ages for deglaciation at the two sampled sites are substantially older than the nearby Dyke (2004) isochrones (Fig. 1), which were not updated in the recent ^{14}C-based Laurentide-Cordilleran deglacial compilation of Dalton et al. (2020). Site B16-1 is ~10 km west of the ~11.5 cal ka isochrone, but the 13.9±0.6 ka deglacial age from six ^{10}Be-dated erratics is ~2.4 kyr older. Similarly, the deglacial age of 12.4±0.5 ka from five ^{10}Be-dated erratics at site B16-2 is ~1.6 kyr older than the Dyke (2004) ~10.8 cal ka BP isochrone, only 10 km to the west. Using a similar approach, Lowell et al. (2021) also found that direct ^{10}Be dates for deglaciation of the southwest sector of the Laurentide Ice Sheet's Labrador Dome are up to several thousand years older than isochrones based on ^{14}C dates (Dyke, 2004; Dalton et al., 2020). Similarly, Norris et al. (in press) suggested that the southwest Laurentide ice sheet retreated from the Cree Lake moraine in northwest Saskatchewan, ~900 km south-southeast of our study area (Fig. 1A), about one thousand years earlier than previously suggested (Dyke, 2004; Dalton et al., 2020). In his synthesis, Dyke (2004) cautioned that there was substantial (~1 kyr) uncertainty associated with the absolute geochronology of deglacial isochrones. Nevertheless, the large differences between our direct uplift-corrected ^{10}Be ages for ice-free conditions and the canonical deglacial history (Bryson et al., 1969; Dyke & Prest, 1987; Dyke, 2004; Dalton et al., 2020) prompt us to consider two key potential sources of error in our analysis.

First, it is possible that uplift-correcting the ^{10}Be exposure ages results in an overcorrection for the effects of decreasing atmospheric depth due to isostatic rebound since deglaciation, as our analysis does not account for potential offsetting atmospheric compression during intervals of cold climate and/or persistent katabatic winds (Staiger et al., 2007; Young et al., 2020). However, the effect of atmospheric compression due to decreased temperature is thought to be minimal for low elevation sites like those considered here (Staiger et al., 2007); in all cases where atmospheric compression changes have been quantitatively and transiently assessed with a full general circulation model, the cumulative effects are minimal, having an impact equivalent to <10 m of elevation change over 10-15 kyrs (Cuzzone et al., 2016; Ullman et al., 2016; Leydet et al., 2018). It is also possible that modeled uplift histories underpinning the exposure age uplift correction are inaccurate and thus potentially over- or under-correct for this effect. However, we explored a reasonable range in earth viscosity parameters (Lambeck et al., 2017) and ice-sheet loading histories. Furthermore, the new ice-sheet model simulations for the uplift correction yield modern uplift estimates that are consistent with geodetic measurements at the closest monitoring station at Yellowknife (Argus et al., 2010; Peltier et al., 2015).

Second, it is also possible that our samples were affected by cosmogenic nuclide inheritance, which would skew the exposure ages older than the true timing of deglaciation. However, inheritance is usually denoted in a suite of surface exposure ages as a long tail towards older ages, which we do not observe in our dataset. Indeed, the sample sets at both sites have remarkably strong internal consistency: after removing one notably young outlier from site B16-2 that had poor AMS counting statistics (Table 1), the MSWD of the sample sets indicates that differences between individual ages at each site are smaller than mean analytical uncertainty.

Consequently, we conclude that our uplift-corrected ^{10}Be ages provide realistic constraints on the timing of northwest Laurentide ice-sheet retreat in the western Slave Craton field area. The ~13.9 ka mean ^{10}Be age at the western site B16-1 shows that the nearby Dyke (2004) ~11.5 cal ka isochrone was already ice-free well before the start of the Younger Dryas. In turn, this requires that the Dyke (2004) ~13.0 and ~12.6 cal ka isochrones further to the west must also be older, consistent with earlier suggestions (Smith, 1992) that the middle reach of the

Mackenzie River drainage system was ice-free prior to the Younger Dryas. Though our new ^{10}Be dates from the western Slave Craton sector of the northwest Laurentide ice sheet only provide a minimum age for opening of the middle Mackenzie River drainage system, the implication of older ages for the Dyke (2004) ~13.0 and ~12.6 cal ka isochrones does not conflict with ^{14}C ages that underpin the chronology of those isochrones, which are, respectively, wood in deltaic sands (13.2–13.6 cal ka BP, I-15020; Smith et al., 1992) and basal gyttja (12.1–12.7 cal ka BP, GSC-3524; MacDonald, 1987) (Fig. 1B). Similarly, our new chronology from the western Canadian Shield is consistent with boulder ^{10}Be exposure dates of ~14.5 ka for deglaciation in the Franklin Mountains (Margold et al., 2019; ~400 km to west; Fig. 1A) and northwest Saskatchewan (Norris et al., in press; ~900 km to south-southeast; Fig. 1A), the latter of which provides important temporal constraints on the opening of a northwest outlet for drainage of Glacial Lake Agassiz (Smith and Fisher, 1993).

The Dyke (2004) northwest Laurentide ice-sheet deglacial chronology includes an acceleration in ice-sheet retreat rate at the start of the Younger Dryas (Fig. 3D) between the 13.0 and 12.6 cal ka isochrones (Fig. 3C) (Dyke, 2004). At the approximate latitude of our ^{10}Be sample sites, this acceleration is expressed as 375 km of retreat in 400 years at a rate of ~830 km kyr^{-1}. In contrast, the direct ^{10}Be deglaciation ages presented here yield an ice-margin retreat rate of 60-100 km kyr^{-1} over 110 km, from 13.9±0.2 ka to 12.4±0.2 ka (Fig. 3C). This time interval spans the Allerød warm period to the Younger Dryas cold period (Fig. 3D). Thus, we find no evidence for a retreat-rate acceleration for the northwest Laurentide ice sheet at the start of the Younger Dryas. Because this purported acceleration at least partly underlies arguments for a northwest Laurentide ice-sheet meltwater forcing of the Younger Dryas cold period (Tarasov & Peltier, 2005), future ice-sheet model simulations should test the extent to which such a possible meltwater forcing would still exist using our new ^{10}Be-based deglacial chronology.

We conclude that the existing deglacial chronology for the northwest sector of the Laurentide ice sheet requires major revision, with tightly clustered ^{10}Be exposure ages showing that deglaciation on the western Slave Craton likely occurred at least 1.5 kyr earlier than suggested by existing compilations (Dyke, 2004; Dalton et al., 2020). Ongoing glacial geochronology research in the Slave Craton region and further to the east (e.g., Campbell et al., 2019; Kelley et al., 2020) will further highlight the need for revision of deglacial chronology for the northwest sector of the Laurentide ice sheet. The strong internal consistency of ^{10}Be boulder exposure ages at these two sites presented here suggests that additional, carefully targeted, ^{10}Be surface exposure dating in the broader Canadian Shield study area will substantially improve the deglacial chronology for this understudied portion of the Laurentide ice sheet and will assist efforts to understand potential linkages to abrupt climate change and global mean sea-level rise.

AUTHOR CONTRIBUTIONS

Conceptualization: AVR, AEC, JRR; Methodology: AVR, AEC, GAM, LT; Investigation: AVR, AEC, GAM, LT, JRR, MWC; Visualization: AVR, AEC; Funding acquisition: AVR, AEC, GAM, LT; Writing – original draft: AVR, AEC; Writing – review and editing: AVR, AEC, GAM, LT, JRR, MWC

DECLARATION OF COMPETING INTERESTS

The authors declare that they have no known competing financial interests or personal relationships that could appear to have influenced the work reported in this paper.

ACKNOWLEDGEMENTS

We thank Tom Chacko (University of Alberta) for supporting fieldwork through his NSERC Northern Research Supplement, and Rick Carlson and Steve Shirey (Carnegie Institution for Science) for facilitating fieldwork at Point Lake (supported by NSF award OCE-1524384). Research was also supported by NSERC Discovery Grants (AVR, GAM, LT) and Northern Research Supplements (AVR), and NSF award OPP-1936880. We thank John Ketchum and

Scott Cairns (Northwest Territories Geological Survey) for logistical support; Sophie Norris for sharing an unpublished manuscript; and Claude Hillaire-Marcel and Jim Teller for comments and suggestions that improved the manuscript.

APPENDIX

The following items appear in the Supplementary Data to this article:

Fig. S1. Oblique aerial photo of site B16-1 (top), and photos of individual boulder erratic samples at site B16-1 annotated with uplift-corrected ^{10}Be exposure ages.

Fig. S2. Oblique aerial photo of site B16-2 (top), and photos of individual boulder erratic samples at site B16-2 annotated with uplift-corrected ^{10}Be exposure ages.

Table S1. Sample information and ^{10}Be concentration data

REFERENCES

Argus, D.F., Peltier, W.R., 2010. Constraining models of postglacial rebound using space geodesy: a detailed assessment of model ICE-5G (VM2) and its relatives. Geophys. J. Int. 181, 697-723. doi: 10.1111/j.1365-246X.2010.04562.x

Balco, G., Stone, J.O., Lifton, N.A., Dunai, T.J., 2008. A complete and easily accessible means of calculating surface exposure ages or erosion rates from ^{10}Be and ^{26}Al measurements. Quat. Geochronol. 3, 174-195. doi:10.1016/j.quageo.2007.12.001

Broecker, W.S., Kennett, J.P., Flower, B.P., Teller, J.T., Trumbore, S., Bonani, G., Wolfli, W., 1989. Routing of meltwater from the Laurentide Ice Sheet during the Younger Dryas cold episode. Nature 341, 318-321. doi:10.1038/341318a0

Bryson, R.A., Wendland, W.M., Ives, J.D., Andrews, J.T., 1969. Radiocarbon isochrones on the disintegration of the Laurentide ice sheet. Arctic Alpine Res. 1, 1-14. doi:10.1080/00040851.1969.12003535

Campbell, J.E., McMartin, I., Normandeau, P.X., Godbout, P.-M., 2019. Report of 2018 activities for the GEM-2 Rae project glacial history activity in the eastern Northwest Territories and the

Kitikmeot and Kivalliq Regions, Nunavut. Geological Survey of Canada Open File 8586, 18 p. doi: 10.4095/314741

Carlson, A.E., 2020. Comment on: Deglaciation of the Greenland and Laurentide ice sheets interrupted by glacier advance during abrupt coolings. Quat. Sci. Rev. 20, 106354. doi: 10.1016/j.quascirev.2020.106354

Carlson, A.E., Clark, P.U., 2012. Ice sheet sources of sea level rise and freshwater discharge during the last deglaciation. Rev. Geophys. 50, RG4007. doi:10.1029/2011RG000371

Carlson, A.E., Clark, P.U., Haley, B.A., Klinkhammer, G.P., Simmons, K., Brook, E.J., Meissner, K.J., 2007a. Geochemical proxies of North American freshwater routing during the Younger Dryas cold event. Proceed. Nat. Acad. Sci. 104, 6556-6561. doi: 10.1073/pnas.0611313104

Carlson, A.E., Clark, P.U., Raisbeck, G.M., Brook, E.J., 2007b. Rapid Holocene deglaciation of the Labrador Sector of the Laurentide Ice Sheet. J. Climate 20, 5126-5133. doi:10.1175/JCLI4273.1

Clark, P.U., Dyke, A.S., Shakun, J.D., Carlson, A.E., Clark, J., Wohlfarth, B., Mitrovica, J.X., Hostetler, S.W., McCabe, A.M., 2009. The Last Glacial Maximum. Science 324, 710-714. doi: 10.1126/science.1172873

Condron, A., Winsor, P., 2012. Meltwater routing and the Younger Dryas. Proc. Natl. Acad. Sci. USA 109, 19,928-19,933. doi:10.1073/pnas.1207381109

Crann, C.A., Patterson, R.T., Crann, C.A., Macumber, A.L., Galloway, J.M., Roe, H.M., Blaauw, M., Swindles, G.T., Falck, H., 2015. Sediment accumulation rates in subarctic lakes: Insights into age-depth modeling from 22 dated lake records from the Northwest Territories, Canada. Quat. Geochronol. 27, 131-144. doi:10.1016/j.quageo.2015.02.001

Cuzzone, J.K., Clark, P.U., Carlson, A.E., Ullman, D.J., Rinterknecht, V.R., Milne, G.A., Lunkka, J.-P., Wohlfarth, B., Marcott, S.A., Caffee, M., 2016. Final deglaciation of the Scandinavian Ice Sheet and implications for the Holocene global sea-level budget. Earth Planet. Sc. Lett. 448, 34-41. doi:10.1016/j.epsl.2016.05.019

Dalton, A.S. et al., 2020. An updated radiocarbon-based ice margin chronology for the last deglaciation of the North American Ice Sheet Complex. Quat. Sci. Rev. 234, 106223. doi:10.1016/j.quascirev.2020.106223.

Dredge, L.A., Ward, B.C., Kerr, D.E., 1995. Surficial Geology, Aylmer Lake, District of Mackenzie, Northwest Territories. Geological Survey of Canada Map 1867A. doi:10.4095/207631

Dyke, A.S., 2004. An outline of North American deglaciation with emphasis on central and northern Canada. Developments in Quaternary Sciences 2B, 373-424. doi:10.1016/S1571-0866(04)80209-4

Dyke, A.S., Prest, V.K., 1987. Late Wisconsinan and Holocene history of the Laurentide Ice Sheet. Geogr. Phys. Quatern. 41, 237-263. doi:10.7202/032681ar

Dyke, A.S., Moore, A., Robertson, L., 2003. Deglaciation of North America. Geological Survey of Canada Open File 1574. doi:10.4095/214399

Johnson, R.G., McClure, B.T., 1976. A model for northern hemisphere continental ice sheet variation. Quat. Res., 6, 325-353. doi:10.1016/0033-5894(67)90001-4

Jones, R.S., Whitehouse, P.L., Bentley, M.J., Small, D., Dalton, A.S., 2019. Impact of glacial isostatic adjustment on cosmogenic surface-exposure dating. Quat. Sci. Rev. 212, 206-212. doi:10.1016/j.quascirev.2019.03.012

Keigwin, L.D., Klotsko, S., Zhao, N., Reilly, B., Giosan, L., Driscoll, N.W., 2018. Deglacial floods in the Beaufort Sea preceded Younger Dryas cooling. Nature Geosci. 11, 599-604. doi:10.1038/s41561-018-0169-6

Kelley, S.E., Ward, B., Briner, J., Ross, M., Normandeau, P., Elliott, B., 2020. The recession of the Laurentide Ice Sheet in southeast Northwest Territories during the Pleistocene-Holocene transition. EGU General Assembly 2020, EGU2020-5410. doi:10.5194/egusphere-egu2020-5410

Kohl, C.P., Nishiizumi, K., 1992. Chemical isolation of quartz for measurement of in-situ - produced cosmogenic nuclides. Geochim. Cosmochim. Acta 56, 3583-3587. doi: 10.1016/0016-7037(92)90401-4

Lambeck, K., Purcell, A., Zhao, S., 2017. The North American Late Wisconsin ice sheet and mantle viscosity from glacial rebound analyses. Quat. Sci. Rev. 158, 172-210. doi:10.1016/j.quascirev.2016.11.033

Lemmen D.S., Duk-Rodkin A., Bednarski J.M., 1994. Late glacial drainage systems along the northwestern margin of the Laurentide Ice Sheet. Quat. Sci. Rev. 13, 805-828. doi:10.1016/0277-3791(94)90003-5

Leydet, D.J., Carlson, A.E., Teller, J.T., Breckenridge, A., Barth, A.M., Ullman, D.J., Sinclair, G., Milne, G.A., Cuzzone, J.K., Caffee, M.W., 2018. Opening of glacial Lake Agassiz's eastern outlets by the start of the Younger Dryas cold period. Geology 46, 155–158. doi:10.1130/G39501.1

Lifton, N., Sato, T., Dunai, T.J., 2014. Scaling in situ cosmogenic nuclide production rates using analytical approximations to atmospheric cosmic-ray fluxes. Earth Planet. Sci. Lett. 386, 149-160. doi: 10.1016/j.epsl.2013.10.052

Love, R., Andres, H.J., Condron, A., Tarasov, L., 2021. Freshwater routing in eddy-permitting simulations of the last deglacial: the impact of realistic freshwater discharge. Clim. Past 17, 2327–2341. doi:10.5194/cp-17-2327-2021

Lowell, T.V., Kelly, M.A., Howley, J.A., Fisher, T.G., Barnett, P.J., Schwartz, R., Zimmerman, S.R.H., Norris, N., Malone, A.G.O., 2021. Near-constant retreat rate of a terrestrial margin of the Laurentide Ice Sheet during the last deglaciation. Geology 49, 1511-1515. doi: 10.1130/G49081.1

MacDonald, G.M., 1987. Postglacial vegetation history of the Mackenzie River basin. Quat. Res. 28, 245-262. doi:10.1016/0033-5894(87)90063-9

Margold, M., Gosse, J.C., Hidy, A.J., Woywitka, R.J., Young, J.M., Froese, D., 2019. The retreat chronology of the western Laurentide Ice Sheet. Geophysical Research Abstracts 21, EGU2019-8344.

McNeely, R., McCuaig, S., 1991. Geological Survey of Canada radiocarbon dates XXIX. Geological Survey of Canada Paper 89-7. doi: 10.4095/132453

McNeely, R., Dyke, A.S., Southon, J.R., 2006. Canadian marine reservoir ages: preliminary data assessment. Geological Survey of Canada Open File 5049. doi:10.4095/221564

Moser, K.A., MacDonald, G.M., 1990. Holocene vegetation change at treeline north of Yellowknife, northwest Territories, Canada. Quat. Res. 34, 227-239. doi:10.1016/0033-5894(90)90033-H

Murton, J.B., Bateman, M.D, Dallimore, S.R., Teller, J.T., Yang, Z., 2010. Identification of Younger Dryas outburst flood path from Lake Agassiz to the Arctic Ocean. Nature 464, 740-743. doi:10.1038/nature08954

Nishiizumi, K., Imamura, M., Caffee, M.W., Southon, J.R., Finkel, R.C., McAninch, J., 2007. Absolute calibration of ^{10}Be AMS standards. Nucl. Instrum. Methods Phys. Res. B 258, 403-413. doi: 10.1016/j.nimb.2007.01.297

Norris, S.L., Garcia-Castellanos, D., Jansen, J.D., Carling, P.A., Margold, M., Woywitka, R.J., Froese, D.G., 2021. Catastrophic drainage from the northwestern outlet of Glacial Lake Agassiz during the Younger Dryas. Geophys. Res. Lett. 48, e2021GL093919. doi: 10.1029/2021GL093919

Norris, S.L., Tarasov, L., Monteath, A.J., Gosse, J.C., Hidy, A.J., Margold, M., Froese, D.G., in press. Rapid retreat of the southwestern Laurentide Ice Sheet during the Bølling-Allerød interval. Geology.

Peltier, W.R., Argus, D.F., Drummond, R., 2015. Space geodesy constrains ice-age terminal deglaciation: the global ICE-6G_C (VM5a) model. J. Geophys. Res.-Sol. Ea. 120, 450-487. doi:10.1002/2014JB011176

Rasmussen, S.O., Andersen, K.K., Svensson, A.M., Steffensen, J.P., Vinther, B.M., Clausen, H.B., Siggaard-Andersen, M.-L., Johnsen, S.J., Larsen, L.B., Dahl- Jensen, D., Bigler, M., Röthlisberger, R., Fischer, H., Goto-Azuma, K., Hansson, M.E., Ruth, U., 2006. A new Greenland ice core chronology for the last glacial termination. J. Geophys. Res.-Atmos. 111, D06102. doi:10.1029/2005JD006079

Reimer, P.J., et al., 2020, The IntCal20 Northern Hemisphere Radiocarbon Age Calibration Curve (0–55 cal kBP). Radiocarbon 62, 725-757. doi:10.1017/RDC.2020.41

Rooth, C., 1982. Hydrology and ocean circulation. Prog. Oceanogr. 11, 131-149. doi:10.1016/0079-6611(82)90006-4

Sharma P., Bourgeois M., Elmore D., Granger D., Lipschutz M.E., Ma X., Miller T., Mueller, K., Rickey, F., Simms, P., Vogt, S., 2000. PRIME lab AMS performance, upgrades and research applications. Nucl. Instrum. Methods Phys. Res. B 172, 112-123. doi: 10.1016/S0168-583X(00)00132-4

Smith, D.G., 1992. Glacial Lake Mackenzie, Mackenzie Valley, Northwest Territories, Canada. Can. J. Earth Sci. 29, 1756-1766. doi:10.1139/e92-138

Smith, D.G., Fisher, T.G., 1993. Glacial Lake Agassiz: The northwestern outlet and paleoflood. Geology 21, 9-12. doi: 10.1130/0091-7613(1993)021<0009:GLATNO>2.3.CO;2

Staiger, J., Gosse, J., Toracinta, R., Oglesby, B., Fastook, J., Johnson, J.V., 2007. Atmospheric scaling of cosmogenic nuclide production: climate effect. J. Geophys. Res.-Sol. Ea. 112, B02205. doi:10.1029/2005JB003811

Stuiver, M., Reimer, P.J., Reimer, R.W., 2020. CALIB 8.2, http://calib.org

Tarasov, L., Peltier, W.R., 2005. Arctic freshwater forcing of the Younger Dryas cold reversal. Nature 435, 662-665. doi: 10.1038/nature03617

Tarasov, L., Peltier, W.R., 2006. A calibrated deglacial drainage chronology for the North American continent: evidence of an Arctic trigger for the Younger Dryas. Quat. Sci. Rev. 25, 659-688. doi:10.1016/j.quascirev.2005.12.006

Tarasov, L., Dyke, A.S., Neal, R.M., Peltier, W.R., 2012. A data-calibrated distribution of deglacial chronologies for the North American ice complex from glaciological modeling. Earth Planet. Sc. Lett. 315-316, 30-40. doi:10.1016/j.epsl.2011.09.010

Ullman, D.J., Carlson, A.E., Hostetler, S.W., Clark, P.U., Cuzzone, J., Milne, G.A., Winsor, K., Caffee, M., 2016. Final Laurentide ice-sheet deglaciation and Holocene climate-sea level change. Quat. Sci. Rev. 152, 49-59. doi:10.1016/j.quascirev.2016.09.014

Upiter, L.M., Vermaire, J.C., Patterson, R.T., Crann, C.A., Galloway, J.M., Macumber, A.L., Neville, L.A., Swindles, G.T., Falck, H., Roe, H.M., Pisaric, M.F.J., 2014. Middle to late Holocene chironomid-inferred July temperatures for the central Northwest Territories, Canada. J. Paleolimnol. 52, 11–26. doi:10.1007/s10933-014-9775-5

Young, N.E., Briner, J.P., Miller, G.H., Lesnek, A.J., Crump, S.E., Thomas, E.K., Pendleton, S.L., Cuzzone, J., Lamp, J., Zimmerman, S., Caffee, M., Schaefer, J.M., 2020. Deglaciation of the Greenland and Laurentide ice sheets interrupted by glacier advance during abrupt coolings. Quat. Sci. Rev. 229, 106091. doi: 10.1016/j.quascirev.2019.106091

Young, N.E., Schaefer, J.M., Briner, J.P., Goehring, B.M., 2013. A ^{10}Be production-rate calibration for the Arctic. J. Quat. Sci. 28, 515-526. doi:10.1002/jqs.2642

FIGURE CAPTIONS

Fig. 1. (A) Map of northern Canada with deglacial isochrones (Dyke, 2004; Dalton et al., 2020). Thick dashed lines mark the mapped ~13.4 cal ka BP (11.5 ^{14}C ka BP) isochrone for the Cordilleran and Laurentide ice sheets; thin dashed lines are deglacial isochrones for the Laurentide ice sheet at 500 ^{14}C-year intervals until 8.9 cal ka BP (8.0 ^{14}C ka BP). Labels are the approximate calendar age associated with each isochrone in cal ka BP. Boulder sampling sites, white dots; ^{14}C-dated sites mentioned in text, squares; Franklin Mountains (FM) site of Margold et al., (2019) and Cree Lake moraine (CLM) site of Norris et al. (in press), diamonds; red line marked A-A’, transect for time-distance and retreat-rate plots in Fig. 3; dotted rectangle, extent of (B). (B) Regional shaded relief map with uplift-corrected ^{10}Be boulder exposure ages at sites

B16-1 and B16-2 (circles). Error-weighted site mean ± internal (external) uncertainty is bolded; rejected outlier marked by asterisk. Also shown are Dyke (2004) 11.5 and 10.8 cal ka BP deglacial isochrones (dashed lines) and previously published ^{14}C date at Acasta Lake. (C) Oblique aerial photograph of site B16-1 (arrow); view to east-northeast. (D) Representative ^{10}Be-dated boulder at site B16-1 (Table 1). Field photographs are provided in Figs. S1, S2.

Fig. 2. Modeled uplift histories and time-averaged postglacial uplift for sites B16-1 (A, C, E) and B16-2 (B, D, F). (A, B) Uplift histories calculated using nine earth model parameter sets (black lines) and the Lambeck et al. (2017) ice model. (C, D) Uplift histories calculated using a single earth model forced by six North America ice sheet model simulations (thin black lines; Tarasov et al., 2012) and two new ice sheet model simulations (following Tarasov et al., 2012) based on Dyke (2004) isochrones modified with the updated ^{10}Be chronology (thick red lines). (E, F) Time-averaged postglacial uplift adjustment for the Lambeck et al. (2017) model results (circles), and the Tarasov et al. (2012) ice sheet simulations (black squares) and Dyke (2004) isochrones modified with the updated ^{10}Be chronology (red squares with outline).

Fig. 3. (A) Uplift-corrected boulder ^{10}Be exposure ages for sites B16-1 (circles) and B16-2 (diamonds). Bars are 1σ external uncertainty envelopes (internal uncertainty plus propagated production rate uncertainty). (B, C) Time-distance diagram (B) and inferred ice margin retreat rate (C) for deglaciation of the northwestern sector of the Laurentide ice sheet along the transect in Fig. 1A, based on direct ^{10}Be deglaciation ages. Purple dots in (B) are error-weighted mean of ^{10}Be ages at each site with internal and external uncertainty errors bars, and the purple bar in (C) represents the range of retreat rates between the two sites. Deglacial isochrones along the transect, following Dyke (2004), are marked by dashed blue lines in (B) and (C). (D) Summit Greenland mean summer air temperature reconstructed from Dye-3 ice core $\delta^{18}O$ (Rasmussen et al., 2006).

Table 1. ^{10}Be sample information.[a]

Sample	Elevation (m)[b]	Uplift correction (m)[c]	Sample thickness (cm)	^{10}Be (atoms g^{-1})	^{10}Be uncertainty (atoms g^{-1})	Uncorrected exposure age (ka)[d]	Uplift-corrected exposure age (ka)[d]
Site B16-1 (65.10 °N, 115.72 °W)							
AVR16-04	470	-111	3	83213	3026	12.8 ± 0.5	14.4 ± 0.5
AVR16-05	470	-111	2	80022	2940	12.2 ± 0.4	13.7 ± 0.5
AVR16-06	470	-111	3.5	78565	3627	12.1 ± 0.6	13.6 ± 0.6
AVR16-07	470	-111	4	81852	3660	12.6 ± 0.6	14.3 ± 0.6
AVR16-08	470	-111	3.5	78799	2521	12.1 ± 0.4	13.7 ± 0.4
AVR16-09	470	-111	3	80852	3728	12.4 ± 0.6	14.0 ± 0.6
						site mean[e]	**13.9 ± 0.2 (0.6)**
Site B16-2 (65.27 °N, 113.27 °W)							
JR16-224	400	-97	0.5	71323	2755	11.5 ± 0.4	12.8 ± 0.5
JR16-225	400	-97	2	67875	2532	11.1 ± 0.4	12.3 ± 0.5
JR16-226	400	-97	3	42854	12908	7.0 ± 2.1	7.8 ± 2.4
JR16-227	400	-97	4	67600	3453	11.2 ± 0.6	12.5 ± 0.6
JR16-228	400	-97	4	65467	3033	10.8 ± 0.4	12.1 ± 0.6
JR16-229	400	-97	3	67393	1595	11.1 ± 0.3	12.3 ± 0.3
						site mean[e]	**12.4 ± 0.2 (0.5)**

[a] Precise sample locations and full mass spectrometry results in Table S1.

[b] Elevation measured in field, m above sea level.

[c] Correction for time-averaged uplift since deglaciation applied to elevation measured in field; see main text.

[d] Lal/Stone age ± internal uncertainty. Ages calculated with: 2.65 g cm^{-3} density; zero erosion rate; and no snow or topographic shielding.

[e] Inverse-error-weighted mean ± internal (external) uncertainty of uplift-corrected exposure ages. Sample JR16-226 is excluded from the Site B16-2 mean. External uncertainty includes propagated production rate uncertainty but not uncertainty related to field elevation measurement, uplift correction, or mean sample thickness.

Figure 1 (full page width)

Click here to access/download;Figure;Reyes_NW-LIS_Fig1_revised.jpg

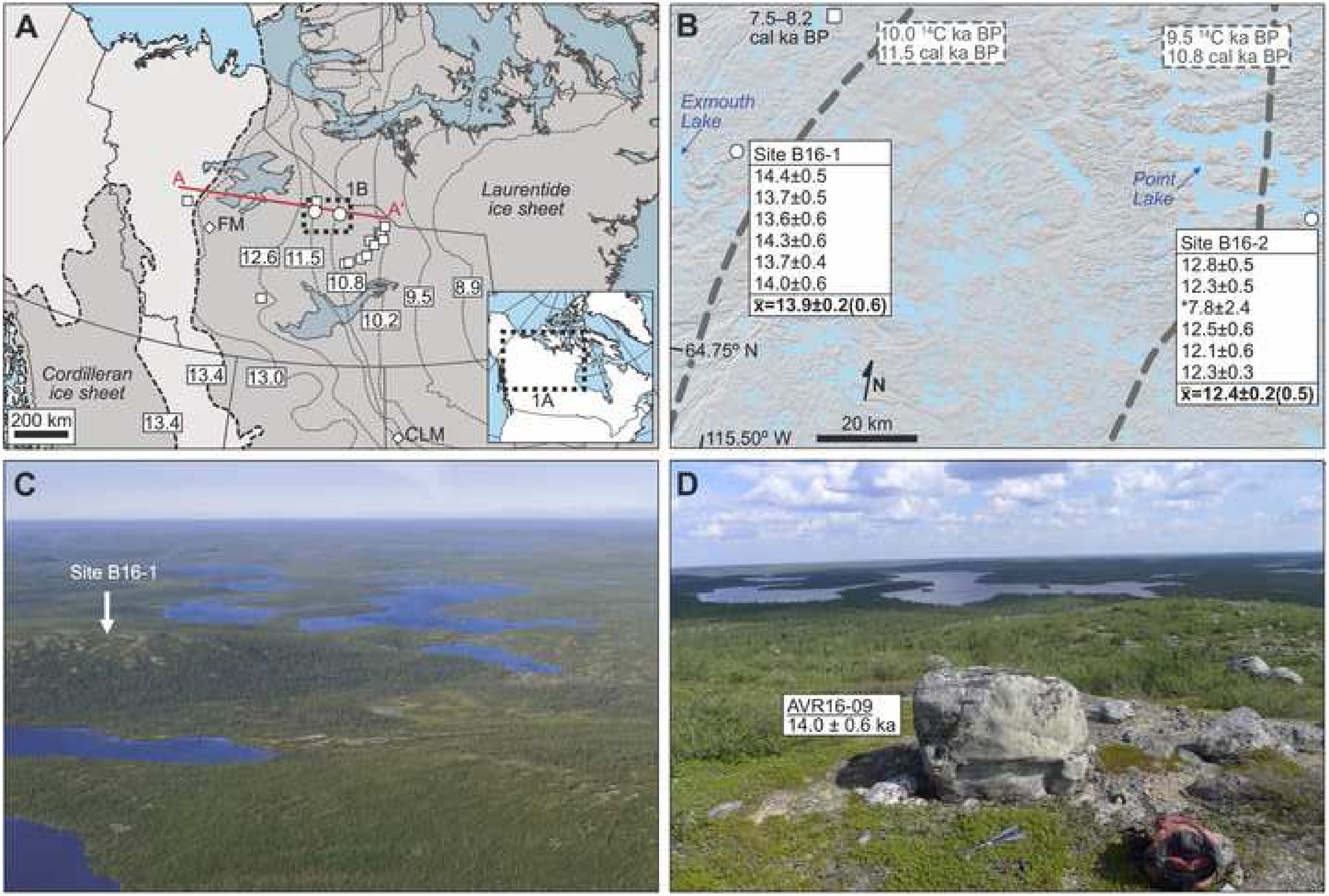

Figure 2 (single column width)

Click here to access/download;Figure;Reyes_NW-LIS_Fig2_revised.jpg

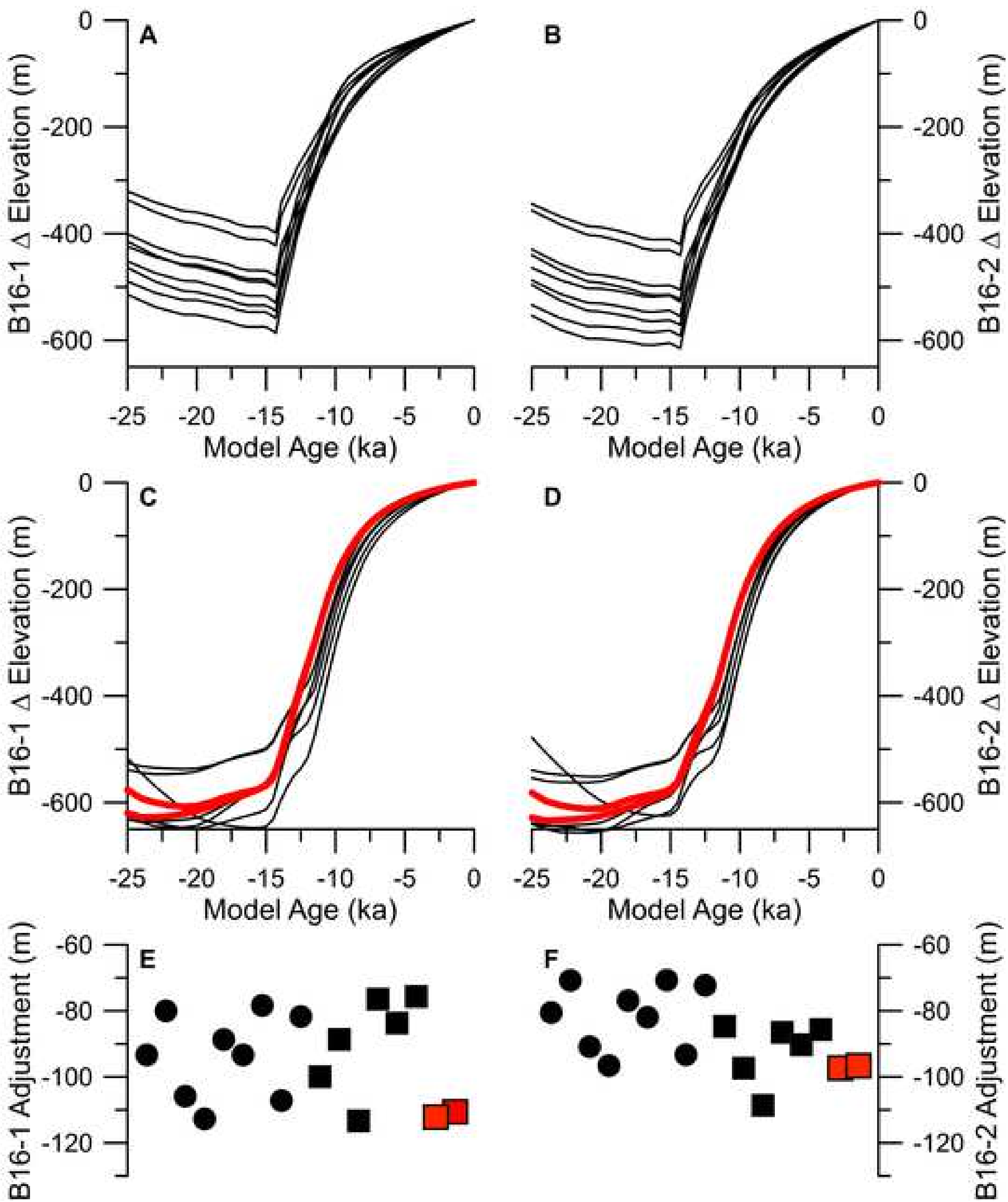

Figure 3 (single column width)

Click here to access/download;Figure;Reyes_NW-LIS_Fig3_revised.jpg

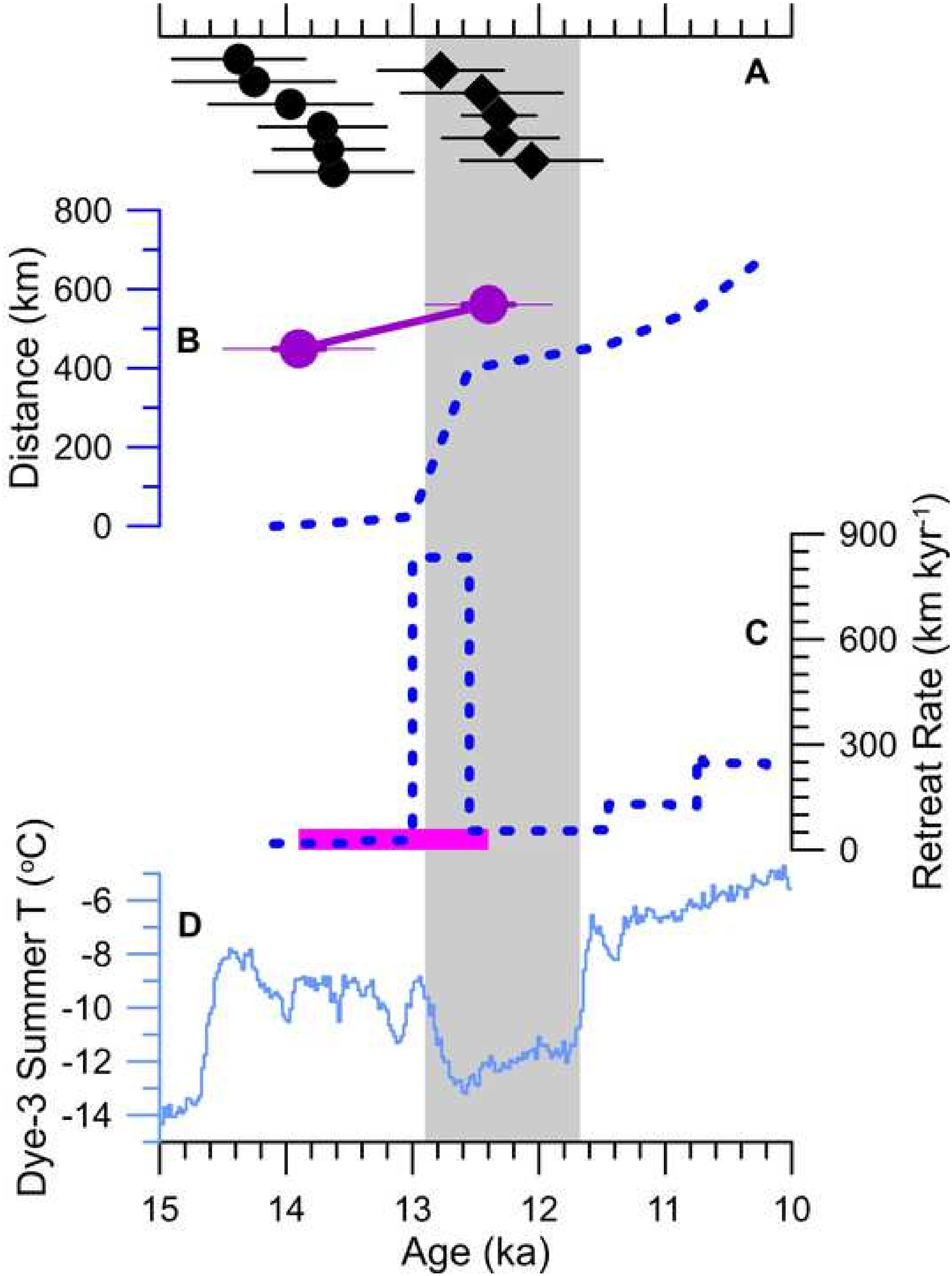

Author contributions for JQSR-D-21-00627 "Revised chronology of northwest Laurentide Ice Sheet deglaciation from ^{10}Be exposure ages on boulder erratics"

Conceptualization: AVR, AEC, JRR; Methodology: AVR, AEC, GAM, LT; Investigation: AVR, AEC, GAM, LT, JRR, MWC; Visualization: AVR, AEC; Funding acquisition: AVR, AEC, GAM, LT; Writing – original draft: AVR, AEC; Writing – review and editing: AVR, AEC, GAM, LT, JRR, MWC

Supplementary table of 10Be data

Click here to access/download
e-Component/Supplementary data
Reyes_NW-LIS_TableS1.xlsx

Supplementary Figs 1 and 2

Click here to access/download
e-Component/Supplementary data
Reyes_NW-LIS_FigsS1S2.pdf